

Statistical Mechanics of Ferromagnetism; Spherical Model as High-Density Limit

R. BROUT*†

Laboratory of Atomic and Solid-State Physics and Department of Physics, Cornell University, Ithaca, New York

(Received November 15, 1960)

It is shown that there is a class of graphs of the Ising model (or Heisenberg model for $T > T_{\text{Curie}}$) which is comprised of cycle graphs plus some excluded volume effects which sum to the spherical model. The spherical model, suitably generalized for $T < T_{\text{Curie}}$, was conjectured in a previous work to be the high-density limit of the Ising model, correct to $1/z$, where z is the number of spins in the range of the exchange potential (not restricted to nearest neighbor interactions). z^3 measures the range of the exchange potential. This is now proved by examining the omitted graphs. The error is shown to be $O(1/z^2)$.

I. INTRODUCTION

IN this paper, we examine and justify the conjecture of the validity of the spherical model to $O(1/z)$ which was set forth in a previous work¹; z is the number of spins in the range of the exchange potential (not restricted to nearest neighbor interactions). We first show that the spherical model corresponds to the summation of cycle diagrams, with a certain class of errors of excluded volume included. Then, it is shown that the class of graphs which is omitted is higher order in $1/z$, completing the proof.

It is rather remarkable that a model first proposed on grounds of simplicity² alone does in fact correspond to a well-defined approximation to a certain physical model. The spherical model apparently possesses many of the analytic features of the Ising and Heisenberg models in a qualitative and semiquantitative way. Further, it offers the possibility of a first-order approximation about which one can develop a more exact theory. In the text it is shown that the spherical model in fact generates a very convenient propagator which includes in a rather accurate way spin-spin correlations. All graphs not included in the spherical model are conveniently reduced to simpler graphs in terms of this propagator alone. Finally, it has been shown recently that a simple extrapolation from quantum spin waves to the spherical model Curie point can be formulated.³ The validity of the extrapolation rests on the above estimate in $1/z$.

We first discuss the error in the remark of I, that cycle graphs with no excluded volume effects included are the $1/z$ graphs.⁴ We confine ourselves for the moment to the case $T > T_c$. For $(T - T_c)/T_c < 1/z$, then cycles of order z start to contribute in an important way to $\ln Z$ and as $T \rightarrow T_c$, cycles of arbitrarily high order contribute. Now if a cycle has order $< z$, it is clear that the number of configuration for which

excluded-volume effects are important is small. This was the basis of the classification of such graphs as $O(1/z^2)$ and smaller in I. Hence the reasoning in I is correct for $(T - T_c)/T_c > 1/z$ and the results quoted there are correct in this temperature range (precisely the temperature range where the problem of inconsistency of I-Sec. IV did not arise). However, for large cycles of order $> z$, the number of configurations where mistakes of excluded volume arise becomes very large and in fact soon dominates the $1/z$ effect due to a restriction on summation. In other words, the number of cycle graphs with dashed line insertions dominates the $1/z$ effect due to restrictions. Thus for $(T - T_c)/T_c < 1/z$, the classification of I breaks down and it becomes necessary to evaluate excluded-volume graphs. It is rather remarkable that the requirement of a consistent treatment of the $1/z$ term, taking into account excluded volume, gives rise to a consistent theory of the Curie point in that the Curie points found from above and below coincide.

II. SPHERICAL MODEL AND EXCLUDED-VOLUME EFFECTS

We first show how the spherical model accounts for the excluded-volume effect mentioned above, in a qualitative fashion. The most convenient formulation of the spherical model is in the two equations of I, Eqs. (5.10) and (5.11)

$$(1/N) \sum_{\mathbf{q}} \{1 - \beta[v(\mathbf{q}) - \delta]\}^{-1} = 1, \quad (2.1)$$

$$\delta = -2E/N, \quad (2.2)$$

which supply an equation for the energy βE in terms of the quantities $\beta v(\mathbf{q})$. This is most easily obtained by writing Eqs. (2.1) and (2.2) as

$$-2\beta E = \sum_{\mathbf{q}} \sum_{n=2}^{\infty} [\beta/(1 + 2\beta|E|/N)]^n [v(\mathbf{q})]^n. \quad (2.3)$$

Solving Eq. (2.3) iteratively then gives the power series in β for $\beta E(\beta)$. We now note that the sum on cycle diagrams without excluded volume effects gives for βE [I-Eq. (4.1)]

$$-2\beta E = \sum_{\mathbf{q}} \sum_{n=2}^{\infty} \beta^n [v(\mathbf{q})]^n. \quad (2.4)$$

* This work has been supported in part by the Office of Naval Research.

† Albert J. Sloan Fellow.

¹ R. Brout, Phys. Rev. **118**, 1009 (1960); hereafter referred to as I.

² T. Berlin and M. Kac, Phys. Rev. **86**, 821 (1952).

³ F. Englert, Phys. Rev. Letters **5**, 102 (1960).

⁴ I owe this remark to Professor Michael Cohen of the University of Pennsylvania.

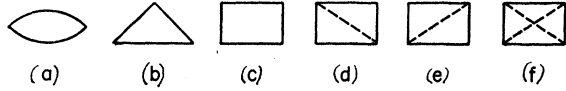


FIG. 1. Cycle diagrams to fourth order.

Thus the effect of the spherical model is to suppress the contribution of the n th cycle by a factor of $(1+2\beta|E|/N)^{-n}$ as compared to the simple result (2.4). (Recall $\beta E < 0$.)

Now in I, it was shown that at $T=T_c$, we have the order of magnitude $\beta_c E/N \sim O(1/z)$ and for $T > T_c$, βE decreases with increasing T . We then see from (2.3) that for $(T-T_c)/T_c < 1/z$, where $\beta E/N = O(1/z)$, the higher order cluster contributions ($n > z$) are indeed given an appropriate suppression factor, whereas for $n < z$ the suppression factor is relatively unimportant. For $(T-T_c)/T_c > 1/z$, then $\beta E/N \rightarrow 0$ quite rapidly and the suppression factor $(1+2\beta|E|/N)^{-n}$ becomes decreasingly important. This is the range of good convergence and only cycles for $n < z$ contribute in an important way; hence the suppression factor need not play an important role. We then see that the spherical model expresses in a qualitative fashion the remarks made in the introduction.

We now will prove that the spherical model sums the class of graphs of the Ising model (or Heisenberg model for $T > T_c$) which comprises cycles plus all dashed line insertions in configurations such that the dashed lines do not cross.

Before constructing the formal proof, we shall indicate the likelihood of the truth of the theorem by power series methods. Solving (2.3) for βE as a power series in β gives the following result. We abbreviate $\langle v^n \rangle = (1/N) \sum_{\mathbf{q}} [v(\mathbf{q})]^n$.

$$-2\beta E/N = \sum_{n=2}^{\infty} \alpha_n \beta^n, \quad (2.5)$$

$$\begin{aligned} \alpha_2 &= \langle v^2 \rangle; & \alpha_3 &= \langle v^3 \rangle \\ \alpha_4 &= \langle v^4 \rangle - 2\langle v^2 \rangle \langle v^2 \rangle; & \alpha_5 &= \langle v^5 \rangle - 5\langle v^2 \rangle \langle v^3 \rangle \\ \alpha_6 &= \langle v^6 \rangle - 6\langle v^4 \rangle \langle v^2 \rangle - 3\langle v^3 \rangle^2 + 7\langle v^2 \rangle^3 \\ \alpha_7 &= \langle v^7 \rangle - 7\langle v^5 \rangle \langle v^2 \rangle - 7\langle v^3 \rangle \langle v^4 \rangle + 28\langle v^2 \rangle \langle v^2 \rangle \langle v^3 \rangle \\ \alpha_8 &= \langle v^8 \rangle - 8\langle v^6 \rangle \langle v^2 \rangle - 8\langle v^5 \rangle \langle v^3 \rangle - 4\langle v^4 \rangle \langle v^4 \rangle \\ &+ 36\langle v^2 \rangle \langle v^2 \rangle \langle v^4 \rangle + 36\langle v^2 \rangle \langle v^3 \rangle \langle v^3 \rangle - 30\langle v^2 \rangle^4. \end{aligned}$$

α_2 and α_3 are two- and three-membered cycles given by Figs. 1(a) and 1(b) for which there are no dashed line insertions possible. α_4 is the sum of contributions of the cycle graph on four vertices with all mistakes included (no dashed lines) plus the two possibilities with diagonal lines. These are Figs. 1(c), 1(d), and 1(e). Figure 1(f) is not included. Rather than go on with the tabulation,

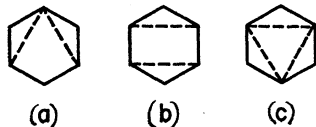


FIG. 2. Contributions to the term $\langle v^6 \rangle^3$ in a sixth-order cycle.

we pick one more sample case. We shall give the diagrams which contribute to the factor $7\langle v^2 \rangle^3$ in α_6 . These are Figs. 2(a), 2(b), and 2(c). There are six Figs. 2(a), three Figs. 2(b), and two Figs. 2(c) of opposite sign from 2(a) and 2(b).

We make one more point here. It has been stated that all graphs whose dashed lines do not cross are included in the spherical model. All such graphs are calculable by convolution, giving rise to the α_n coefficients of (2.5). This is not to say that all graphs obtainable by convolution are counted by the spherical model. Thus in eighth order, Fig. 3(a) is included and 3(b) is not included even though both have the same value. This is discussed in detail in Sec. III.

Now we turn to the formal proof.⁵ It is our aim to evaluate the contribution of certain cycle diagrams to βE for $T > T_c$. This is given by

$$-2\beta E/N = \sum_{n=1}^{\infty} \beta^{n+1} \sum'_{i_1 \dots i_n} v(i_1) v(i_1 i_2) \dots v(i_n 1). \quad (2.6)$$

The prime over the second summation means that the sum is over those cycle graphs which have dashed line insertions with no crossings. In what follows we shall consider as distinct each one of the $n!$ orderings of the indices $i_1 \dots i_n$ (so that the reflection symmetry of a

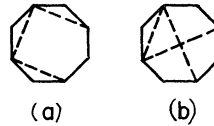


FIG. 3. Contribution to an eighth-order cycle. (a) Contributes to spherical model. (b) Does not contribute to spherical model.

cycle is given up). Define the "irreducible" quantity β_k as the total contribution from all possible orderings of k particles in a cycle of order $k+1$ with *no* dashed line insertions. The point 1 is fixed. Thus

$$\begin{aligned} \beta_k &= \beta^{k+1} k! \sum'_{i_1 \dots i_k} [v(1i_1) \dots v(i_k 1)] \\ &= k! (1/N) \sum_{\mathbf{q}} [\beta v(\mathbf{q})]^{k+1}. \end{aligned} \quad (2.7)$$

Define a "reducible" quantity b_l as the total contribution of all cycles of $(l+1)$ particles (with the position of particle 1 fixed) including all insertions of dashed lines such that the dashed lines do not cross. With this definition

$$b_l = \beta^{l+1} l! \sum'_{i_1 \dots i_l} v(1i_1) \dots v(i_l 1), \quad b_0 \equiv 1, \quad (2.8)$$

where the prime means the same here as in (2.6). We have according to (2.6)

$$-2\beta E/N = \sum_{l=1}^{\infty} (b_l/l!). \quad (2.9)$$

Now consider a given graph contributing to b_L . For

⁵ The work here is inspired by the recent elegant combinatorial approach to statistical mechanics of E. E. Salpeter, *Ann. Phys.* **5**, 183 (1958); and E. Meeron, *J. Phys. Fluids* **1**, 139 (1958).

the moment we take graphs which are comprised of a "skeleton" irreducible part comprising k vertices ($k < L$) and the particle 1 plus reducible parts which are articulated on to each one of the vertices. A convenient graphical notation is obtained by drawing a set of vertices connected by dashed lines as a single vertex corresponding to the fact that a dashed line is a δ function. For example, in the new notation Fig. 4(a) becomes Fig. 4(a'), Fig. 4(b) becomes 4(b'), and Fig. 4(c) becomes Fig. 4(c'). In this new notation, we draw for example a contribution to b_L for $L=11$ in Fig. 5(a). For this case we have $k=4$. To vertex (1) is articulated no cluster. To vertex (2) is articulated two clusters of orders two and three ($l=1$ and 2, respectively). To vertex (3) is articulated no cluster and to vertex 4 is articulated one cluster of order five ($l=4$). The total contribution of such a configuration to b_{11} is obtained by summing on all possible contributions which have the form of Fig. 5(a). For example one would add Fig. 5(b) to Fig. 5(a). The result of this grouping is to convert each of the figures articulated on to the vertices of an irreducible skeleton into a sum of reducible graphs. Thus, associated with such a particular articulated portion of l points, in addition to the vertex of the irreducible skeleton itself is a factor $-b_l$.

We now calculate the total contribution to b_L due to a particular splitting up of the L particles with k particles in the irreducible skeleton (in addition to the given particle 1), l_1^1 particles grouped into a cluster of order (l_1^1+1) articulated to vertex 1, l_1^2 particles grouped into a cluster of order (l_1^2+1) articulated to vertex 1, \dots , $l_1^{\nu_1}$ particles grouped into a cluster of order $(l_1^{\nu_1}+1)$ articulated to vertex 1, \dots , l_i^j particles grouped into a cluster of order (l_i^j+1) articulated to vertex i ($i=1, 2, \dots, k+1$); the superscript j labels which cluster articulated to i is in question.

We write down the answer to this problem and justify each factor in the succeeding paragraph.

$$\frac{L!}{k!} \beta_k \prod_{i=1}^{k+1} g_i \left(\frac{-b_{l_i^1}}{l_i^1!} \right) \dots \left(\frac{-b_{l_i^{\nu_i}}}{l_i^{\nu_i}!} \right). \quad (2.10)$$

The factor $[L!/k! \prod_i (l_i^1!) \dots (l_i^{\nu_i}!)]$ is merely the number of ways to achieve the grouping in question. The factor β_k is the contribution from the k skeleton particles and particle 1. Each of the factors $-b_{l_i^j}$ is the contribution from the articulation of an (l_i^j+1) cluster on to point i in the skeleton. The factor g_i is a further combinatorial effect describable as follows. On to vertex i a certain number ν_i of clusters are articulated. These are of various orders l_i^j ($j=1, \dots, \nu_i$). Let there be m_1^i clusters for which l_i^j is 1, m_2^i clusters for which l_i^j is 2, etc. Then

$$\sum_{j=1}^{\nu_i} m_j^i = \nu_i.$$

The number of ways to articulate these clusters on to

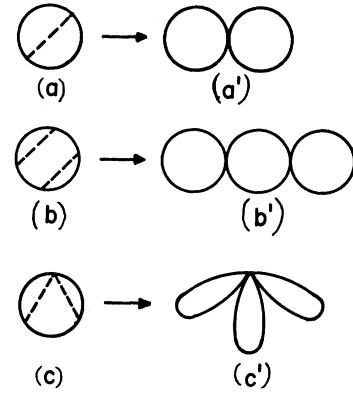


FIG. 4. New notation for dashed line graphs.

point i is g_i :

$$g_i(l_i^1, \dots, l_i^{\nu_i}) = \nu_i! / m_1^i! \dots m_{\nu_i}^i!. \quad (2.11)$$

We now calculate the factor which arises from all the graphs for which there are ν_i clusters articulated on to point i . This is clearly

$$\sum_{l_i^1=1}^{\infty} \dots \sum_{l_i^{\nu_i}=1}^{\infty} g_i(l_i^1, \dots, l_i^{\nu_i}) \left(\frac{-b_{l_i^1}}{l_i^1!} \right) \dots \left(\frac{-b_{l_i^{\nu_i}}}{l_i^{\nu_i}!} \right). \quad (2.12)$$

Making use of the fact that (2.11) is the multinomial coefficient, (2.12) is easily summed to

$$(-1)^{\nu_i} [\sum_{l=1}^{\infty} b_l / l!]^{\nu_i} = (-1)^{\nu_i} (2\beta |E|/N)^{\nu_i}. \quad (2.13)$$

Hence the sum of all clusters articulated on to the vertex i is

$$1 + \sum_{\nu=1}^{\infty} (-1)^{\nu} (2\beta |E|/N)^{\nu} = [1 + 2\beta |E|/N]^{-1}. \quad (2.14)$$

Thus the sum of all diagrams whose skeleton diagram is of order k where there are all possible diagrams articulated on to each vertex i ($i=1, \dots, k+1$) is

$$\beta_k / k! [1 + 2\beta |E|/N]^{-(k+1)}. \quad (2.15)$$

Summing on k we find

$$\begin{aligned} -2\beta E/N &= \sum_{k=1}^{\infty} \beta_k [1 + 2\beta |E|/N]^{-(k+1)} \\ &= \sum_{n=2}^{\infty} \sum_{\mathbf{q}} [\beta v(\mathbf{q})]^n / [1 + 2\beta |E|/N]^n, \end{aligned} \quad (2.16)$$

thereby proving the theorem.

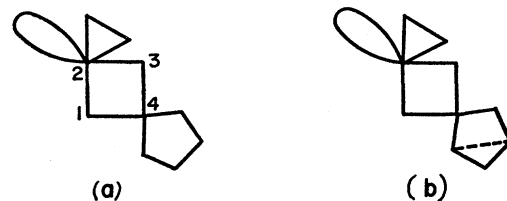


FIG. 5. Contributions to b_l for $l=1, k=4$.

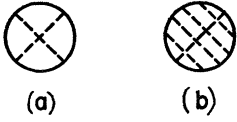


FIG. 6. Sample single cross-linked graphs.

From the analysis of I, Sec. VI, it is seen that this proof holds equally well in the Heisenberg model for $T > T_c$ and zero magnetic field.^{5a}

For the Ising model and $T < T_c$, the work of I, shows that the graphs which arise in $1/z$ are "generalized cycles" which merely changes the spin factor from 1 to $(1-R^2)^n$. The spatial factors, however, are the same. Since the above work is concerned with spatial factors only, we then have found the class of graphs for $T < T_c$ which corresponds to the generalized spherical model with R fixed as given in I.

III. HIGH-DENSITY LIMIT

We show that cycle diagrams not included in the spherical model (i.e., those with crossed dashed lines) contribute higher order in $1/z$. To understand why this is so, consider the general topological configuration of Figs. 1(e) and 1(f). It is clear that the space which may be covered in 1(f) is considerably less than that of 1(e). If z is large, this means that there will not be as many of 1(f) as of 1(e). As an example, we will first sum all diagrams with one pair of crossed lines. Schematically, this is represented by the diagram of Fig. 6(a). Between points 1 and 2, there may appear arbitrarily many bonds and dotted lines. The sum of all such diagrams is equivalent to the evaluation of $\langle \mu_1 \mu_2 \rangle$ in the spherical model where 2 is at a given distance from 1. We call this function g_{12} . Its value is [see I, Eq. (5.10) ff.]

$$g_{12} = \sum_{\mathbf{q}} g(\mathbf{q}) \exp[i\mathbf{q} \cdot (\mathbf{R}_1 - \mathbf{R}_2)], \quad (3.1)$$

$$g(\mathbf{q}) = \beta v(\mathbf{q}) / [1 - \beta w(\mathbf{q})]; \quad w(\mathbf{q}) = v(\mathbf{q}) - \delta. \quad (3.2)$$

This is slightly different from the value given in I, where $g(q) = 1/[1 - \beta w(\mathbf{q})]$. The expression (3.2) has the constant $1/(1 + \beta\mu)$ subtracted from this value. This only affects g_{12} at $R=0$ which is not pertinent to the present calculation. For the case $R_1 = R_2$, it is easy to see that diagram 6(a) goes like $(\beta E)^3 (d\beta E/d\beta) = O(1/z^3)$. The value (3.2) is the one directly obtained by graph summation and is the more appropriate one. The evaluation of the energy $= \sum_{\mathbf{q}} [g(\mathbf{q})v(\mathbf{q})]$ is not affected by which form is adopted since $\sum_{\mathbf{q}} v(\mathbf{q}) = 0$.

It is proved in the Appendix that diagram 6(a) gives a contribution to $2\beta E/N$ equal to

$$\sum_2 \beta (\partial g_{12} / \partial \beta) g_{21} g_{12} g_{21} = (\beta/4) (\partial / \partial \beta) \sum_2 g_{12}^4. \quad (3.3)$$

This is conveniently evaluated by Fourier transforms.

^{5a} Note added in proof. The argument given in I is only correct for simple cycles. Once indices duplicate, there are commutator problems which render the above statement incorrect as it stands. A more complete report on this problem and its relation to spin wave interaction will be forthcoming.

Accordingly we analyze $g(\mathbf{q})$ given by (3.2) at $T = T_c$ since the maximum value of all functions is attained at this temperature. At $T = T_c$, the behavior of $g(\mathbf{q})$ is given by

$$g(\mathbf{q}) \sim \beta_c v(0) / z^3 q^2 \sim 1/z^3 q^2, \quad |\mathbf{q}| < z^{-1/2}; \quad (3.4)$$

$$g(\mathbf{q}) \sim 0, \quad |\mathbf{q}| > z^{-1/2}, \quad (3.5)$$

and in configuration space, since $g(R=0) = \beta\delta$, we have

$$g \sim 1/z, \quad 0 < R < z^{1/2}; \quad (3.6)$$

$$g \sim 1/z^3 R, \quad R > z^{1/2}. \quad (3.7)$$

We may similarly analyze $\beta \partial g_{12} / \partial \beta$, the Fourier transform of which we call $g'(q)$. This is shown in the Appendix to be

$$g'(\mathbf{q}) = \beta v(\mathbf{q}) / [1 - \beta w(\mathbf{q})]^2 = \frac{\beta_c v(\mathbf{q})}{\beta_c^2 [v(0) - v(\mathbf{q})]^2}; \quad T = T_c. \quad (3.8)$$

It appears from (3.8) that $g'(q)$ has an infrared divergence at $q=0$. This would be serious, but is avoided because of the saddle-point condition of the spherical model in the following way. Consider an integral of the form $\int f(\mathbf{q}) g'(\mathbf{q}) d\mathbf{q}$ such that $f(q=0)$ exists. The saddle point condition is

$$1 = (1/N) \sum_{\mathbf{q}} [1 - \beta w(\mathbf{q})]^{-1}, \quad (3.9)$$

which upon differentiation is

$$\sum_{\mathbf{q}} [\partial \beta w(\mathbf{q}) / \partial \beta] / [1 - \beta w(\mathbf{q})]^2 = 0. \quad (3.10)$$

Now

$$\lim_{\beta \rightarrow \beta_c} [\partial \beta w(\mathbf{q}) / \partial \beta] = v(0) - (\partial \beta \delta / \partial \beta) \equiv \alpha \neq 0. \quad (3.11)$$

The infrared divergence of (3.10) cancels out. We then see that a subtraction procedure is available:

$$\begin{aligned} \int f(\mathbf{q}) g'(\mathbf{q}) d\mathbf{q} &= \int f(\mathbf{q}) \frac{\beta v(\mathbf{q})}{[1 - \beta w(\mathbf{q})]^2} d\mathbf{q} \\ &= \int \frac{d\mathbf{q}}{[1 - \beta w(\mathbf{q})]^2} \{ \beta v(\mathbf{q}) f(\mathbf{q}) \\ &\quad - [\beta v(0) f(0) / \alpha] (\partial \beta w(\mathbf{q}) / \partial \beta) \}. \end{aligned} \quad (3.12)$$

Since we generally will deal with $f(\mathbf{q})$ an even function, the curly bracket in (3.12) is of $O(q^2)$, thereby cancelling the infrared divergence. Thus as far as order of magnitude arguments at small q (large R) are concerned, it suffices to replace $\beta \partial g / \partial \beta$ by g since the property (3.4) and hence (3.7) holds for the former as well as the latter quantity once the subtraction procedure is adopted. At small R , however, this is not the case, since as seen from (3.12), $v(\mathbf{q})$ is no longer a factor; hence there is no cutoff at $q = O(z^{-1/2})$.

With the above remark, we first calculate $\sum_2 g_{12}^4$

and then discuss the appropriate modifications to evaluate (3.3). Using (3.6), we have⁶

$$\sum_2 g_{12}^4 \sim \frac{1}{z^4} \int_0^{z^{\frac{1}{2}}} R^2 dR + \frac{1}{z^{\frac{8}{3}}} \int_{z^{\frac{1}{2}}}^{\infty} dR/R^2 \sim 1/z^3. \quad (3.13)$$

For the calculation of $g_{12}^3(dg_{12}/d\beta)$, the above discussion has shown that the second term is $1/z^3$; however, at small R we have $\beta(dg/d\beta) \cong \sum_{\mathbf{q}} \beta v(\mathbf{q})/[1-\beta w(\mathbf{q})]^2$. It is difficult to evaluate this expression exactly; however it certainly varies between $O(1)$ and $O(1/z)$, probably more likely being of $O(1)$, like the specific heat. This is obtained from the use of (3.12) with $f(q) = \beta v(q)$, the upper limit of this integral being independent of z , we expect $O(1)$. We then find

$$\sum \beta(dg_{12}/d\beta)g_{12}^3 \sim O(1/z^2). \quad (3.14)$$

We now proceed to sum all graphs of the form (6b). In the Appendix these are shown to be

$$\sum_{n=1}^{\infty} (-1)^{n+1} \sum_{i_1 \dots i_n} (dg_{i_1 i_1}/d\beta)g_{i_1 i_1}g_{i_1 i_2}^2 \dots g_{i_n i_n}^2. \quad (3.15)$$

Again we first will study

$$\sum_{n=1}^{\infty} (-1)^{n+1} \sum g_{i_1 i_1}^2 \dots g_{i_n i_n}^2$$

and then show how to modify this to obtain an estimate for (3.15). Let the Fourier transform of g_{12}^2 be $G(\mathbf{q})$; then we have

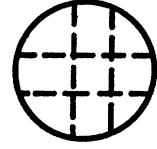
$$\begin{aligned} \sum_{n=1}^{\infty} (-1)^{n+1} \sum_{i_1 \dots i_n} g_{i_1 i_1}^2 \dots g_{i_n i_n}^2 &= \frac{1}{N} \sum_{\mathbf{q}} \sum_{n=2}^{\infty} (-1)^n G^n(\mathbf{q}) \\ &= (1/N) \sum_{\mathbf{q}} G^2(\mathbf{q})/[1+G(\mathbf{q})]. \end{aligned} \quad (3.16)$$

From Eqs. (3.6) and (3.7) it is seen that the function $[1+G(\mathbf{q})]^{-1}$ is well behaved for all \mathbf{q} and $G(\mathbf{q})$ is higher order than $1/z$. Because of this, it may effectively be replaced by unity and the estimate (3.13) applies to (3.16). A check on this statement is made by noting that for small q we have $G(\mathbf{q}) \sim (1/qz^{4/3})$. Substituting into (3.16) and integrating to z^{-3} gives $(1/z^3)[1+(1/z) \times \ln(1/z)]$. Further, for small R , $g^2(R) \sim 1/z^2$, so that for $q > z^{\frac{1}{2}}$, there can be no trouble either. Finally the discussion after (3.13) still holds for the present case and therefore leads to the statement that the sum of all graphs of type (6b) is $O(1/z^2)$.

The next set of cycles to consider is that of Fig. 7 with two sets crossing. Unlike the set of Fig. 6 this set cannot be summed analytically. However, the following argument applies. Introducing one more crossing as in Fig. 7 introduces two extra g factors and one extra integration. From our previous experience (e.g., Eq.

⁶ We replace all sums by integrals. This is permissible to calculate orders of magnitude. The lower limit in (3.13) should be the lattice distance rather than zero. This also however, does not affect the estimate.

FIG. 7. Sample double cross-linked graph.

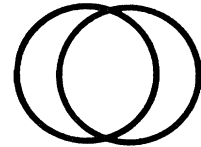


3.13) it is seen that each factor g introduces a factor of $1/z$ and each integration a factor of z . Hence Fig. 7 will introduce one extra factor of $1/z$ compared to those of Fig. 6. This argument continues—the more crossings, the higher the order in $1/z$.

Other diagrams which should be reconsidered are those which are not included in the cycle approximation. For example, there are the ladder diagrams of reference I (e.g., Fig. 4(d) of I). Summation over these ladders⁷ replaces the function βv_{ij} by $\tanh \beta v_{ij} \cong \beta v_{ij} + O(1/z^3)$ at $\beta = \beta_c$. Hence these can be neglected. Similarly there are diagrams like Fig. 8 which itself is obviously higher order in $1/z$. Such diagrams have the same topological structure as diagrams with crossed dashed lines [i.e., Fig. 8 and Fig. 6(a) have the same topological structure]. Since it has been shown that the order of magnitude of the crossed dashed lines is of higher order in $1/z$, it follows that the same is true for the graphs of overlapping cycles, of which Fig. 8 is an example.

Finally we return to the point made earlier: that some graphs in the spherical model are included while others of the same magnitude are not [e.g., Figs. 3(a) and 3(b)]. From the derivation in Sec. II, it is seen that the set of graphs for which more than one reducible cluster is articulated on to a vertex of the irreducible skeletons changes the factor $(1-2\beta E/N)^k$ to $(1+2\beta E/N)^{-k}$. However, since $\beta E/N \sim O(1/z)$, this is an unnecessary refinement. In fact the energy need only be calculated to $1/z$ in order to get the Curie point to $1/z$; i.e., if the suppression factor is $(1-2\beta|E|/N)$ rather than $(1+2\beta|E|/N)^{-1}$ we would obtain $kT_c = v(0)[1-2E/NkT_c] \cong [v(0)-2E/N+O(1/z^2)]$ where $2E/NkT_c$ need only be calculated to $O(1/z)$. However, it would be more consistent to calculate βE to $O(1/z^2)$ in the spherical model in order to exhibit the same singularity for all thermodynamic functions. With this thought in mind we now observe that Fig. 3(a) contributes to a refinement of the spherical model in $O(1/z^3)$. Hence it did not have to be used in the high-density proof. All that is claimed is that the coefficient of $1/z$ in the spherical model is the same as the coefficient of $1/z$ in the Ising (or Heisenberg for $T > T_c$)

FIG. 8. Sample overlapping cycles.



⁷ In fact this is the basis of the method of Kac and Ward on the two-dimensional Ising model [M. Kac and J. Ward, Phys. Rev. 88, 139 (1952)].

model. On this point, it is a matter of indifference whether Fig. 3(a) is included or not.

In reference I, a considerable issue was made about the fact that the Curie points did not coincide when obtained from above (divergence in C_v) or below (confluence in root of $R=0$ or alternatively divergence of χ). In the Gaussian model this relative discrepancy was $O(1/z)$. We now see that the spherical model guarantees kT_c to $O(1/z)$ and thus we have the right to demand of it that there be agreement to $O(1/z)$. It is the virtue of the spherical model, that it sums just those terms of higher order in $1/z$ to lead to perfect agreement. However, the value of kT_c so obtained should still be regarded as having a relative error in $1/z^2$. Further, the singular analytic behavior of thermodynamic function for finite $1/z$ is by no means guaranteed by the spherical model since the coefficient of $1/z^2$ may have entirely different analytic properties at $T=T_c$ from the coefficient of $1/z$. Even for small $1/z$, it is possible that sharper singularities in the coefficient of $1/z^2$ and higher orders might dominate the term in $1/z$ very close to the Curie point.

One final point is the necessity of having to sum cycle diagrams in the order given in the paper. Had we first not taken the spherical model diagrams, but rather only cycles with no excluded-volume effects included (Gaussian model), then the infrared divergence of (3.8) could not have been eliminated. We would have been led to a spurious infinity in the same way that the Gaussian model leads to infinite C_v at $T=T_c$. The elimination of this infinity comes from the no-crossing rule regrouping. The very fact of the convergence obtained in this manner leads one to conjecture on the mathematical necessity of the type of regrouping considered here. In any case, one's confidence in the spherical model is enhanced thereby.

APPENDIX

Consider a special diagram of the form Fig. 6(a), such that between the vertices connected by dashed lines there are $n_1, n_2, n_3,$ and n_4 vertices in all orders where $n_1 \neq n_2 \neq n_3 \neq n_4$. The total number of ways to lay the crossed lines to pick up all such splits is the number of ways to lay down, say point 1 (where by definition n_1 is the number of points to the right of 1), multiplied by the number of ways to arrange the other three groups. Thus

$$[\text{Number of crossed line graphs splitting a cycle into } n_1, n_2, n_3, n_4] = 3!(n_1+n_2+n_3+n_4). \quad (\text{A.1})$$

This combinatorial factor is multiplied by the contribution of each of the segments, i.e., n_1 factors of $\beta v/(1+\beta\delta)$ from 1 to 2, etc. Now the number of ways that such factors come up in $(\partial g_{12}/\partial\beta)g_{23}g_{34}g_{41}$ is

calculated as follows. If n_1 factors come up in $\partial g_{12}/\partial\beta$, this gives a factor n_1 from differentiation of β^{n_1} (it is understood that δ is not to be differentiated); the distribution of n_2, n_3, n_4 in the remaining factors comes up in $3!$ ways. Similarly for n_2 factors in $\partial g_{12}/\partial\beta$, etc. Thus (A.1) is accounted for.

Similar arguments are easily carried out if two or more of the n_i 's are equal. For example, if two n_i 's are equal, the number of dotted line configurations is $3(2n+n_2+n_3)$. The number of ways that this distribution comes up in $(\partial g_{12}/\partial\beta)g_{23}g_{34}g_{41}$ is calculated as follows: For n bonds in $\partial g_{12}/\partial\beta$, the total number of ways to achieve this is $3!$ which is then multiplied by n_2 or n_3 , respectively. The result on adding is $(3!n) + 3(n_1+n_2)$.

Clearly the same argument applies for general diagrams of the type Fig. 6(b). Here the number of ways to lay down configurations for arbitrary splits $\{n_i\}$ is $(\sum_{i=1}^v n_i)(v-1)!$ for v segments and all n_i different. This is precisely the factor arising in $(\partial g_{12}/\partial\beta) \dots g_{v1}$ from such splits. For some n_i the same, it is easily verified that the result is still valid.

We complete this Appendix by proving Eq. (3.8). We have, on summing spherical model graphs,

$$g_{12}(\mathbf{q}) = (1+\beta\delta)^{-2}[\beta v(\mathbf{q}) + \beta v(\mathbf{q})(1+\beta\delta)^{-1}\beta v(\mathbf{q}) + \dots] = [\beta v(\mathbf{q})/(1+\beta\delta)](1/[1-\beta w(\mathbf{q})]). \quad (\text{A.2})$$

Remembering however, that for the graphs in question with various g_{ij} attached to one another, that the common vertex has only one set of articulated reducible parts, not two.

Hence one should only articulate reducible graphs on to one end of a g bond and not to each end as in (A.2). Therefore the result (A.2) must be multiplied by $(1+\beta\delta)$. Finally we must differentiate the result with respect to β , ignoring however the dependence of $\beta\delta$ on β .

$$\beta \partial g_{12}/\partial\beta = [\beta v(\mathbf{q})/(1+\beta\delta)] + 2[\beta v(\mathbf{q})/(1+\beta\delta)]^2 + \dots = (1+\beta\delta)\beta v(\mathbf{q})/[1-\beta w(\mathbf{q})]^2 = \beta v(\mathbf{q})/[1-\beta w(\mathbf{q})]^2 [1+O(1/z)]. \quad (\text{A.3})$$

It is the form (A.3) that is used in the text.

ACKNOWLEDGMENTS

I should like to thank Dr. Carson Mark for his kind hospitality during my stay as summer consultant at Los Alamos Research Laboratory where this work found its beginnings.

It is with pleasure and gratitude that I acknowledge that the stimulus for the line of research followed in this paper came from a cogent critical remark of Professor Michael Cohen⁴ dealing with the previous work¹ in this series.